Pools of ions trapped below the surface of superfluid helium

1999 J. Phys.: Condens. Matter 11 7737

(http://iopscience.iop.org/0953-8984/11/40/306)

J. Phys.: Condens. Matter **11** (1999) 7737–7750. Printed in the UK PII: S0953-8984(99)02441-8

Pools of ions trapped below the surface of superfluid helium

C I Pakes and P L Elliott
School of Physics and Astronomy, University of Birmingham, Birmingham B15 2TT, UK

Received 9 March 1999

Abstract. Pools of ions trapped below the surface of superfluid helium form an ideal arena for the study of the fascinating properties of two-dimensional classical Coulomb solids and liquids. This system can support many different families of collective motion, and furthermore exhibits interesting mode-coupling effects; both of these features are employed to probe its behaviour. A description is given of some of the work that has been of interest over the past few years, focusing in particular on our understanding of the crystalline phase.

1. Introduction

Two-dimensional sheets of either positive or negative ions can be trapped just below the surface of superfluid ^{4}He. This system has been of great interest to the group of Professor W F Vinen at the University of Birmingham since the early 1980s, and an extensive programme of research studying its behaviour has revealed many interesting properties concerning both the physics of superfluid helium and that of the two-dimensional classical Coulomb crystals and fluids that may be formed from arrays of trapped ions. It is the second of these topics with which we are particularly concerned in this paper, which is intended to be an introductory discussion to illustrate some of the issues studied over the last few years of the research programme.

We shall begin by describing the nature of the two types of charged particle, or 'ion', that can be produced in liquid helium, explain how such particles can be trapped below the free surface of the liquid and furthermore describe the characteristics of the ion pools created by making use of this trapping mechanism (section 2). Our experiments are carried out in the temperature range 10–200 mK, for which it is found that the motion of the ions suffers from very little friction. This makes the system ideal for the study of collective modes of oscillation, which has yielded almost everything we know about the physics of the pools. In particular, much work has been done towards achieving an understanding of the different phases within which the pools may exist; within the limited treatment of this paper we shall deal specifically with results related to the two-dimensional classical Coulomb (Wigner) crystal, which forms below a melting temperature, T_m, of typically 100 mK. We shall consider the study of magnetoplasma modes in the trapped pools in section 3, including the different classes of edge magnetoplasma mode which have been observed by exploiting a non-linear coupling which has been shown to exist between different modes. The crystalline phase supports, in addition, the propagation of transverse shear modes, the observation of which is discussed in section 4. Section 5 explores the damage and annealing of the ion crystal, these processes being, respectively, imposed and monitored using the observed transverse shear mode response. In section 6 we show that quantized capillary waves (ripplons) on the helium surface also may be employed as a probe of the structure of the underlying Wigner solid, giving rise to a novel

0953-8984/99/407737+14$30.00

technique of 'capillary-wave crystallography', which has allowed us to investigate important fundamental issues regarding the nature of the crystalline state in two dimensions. Finally, our concluding remarks are contained in section 7.

2. Ions in liquid helium and the trapping mechanism

The charged particles with which we are concerned are of two types, positive and negative, which are formed, respectively, by field ionization and emission at a sharp tungsten tip held at a high electrostatic potential. The positive 'ion' consists of a He_2^+ ion surrounded by a solid 'snowball' of about 25 helium atoms, which results from an electrostrictive increase in the helium density around the ion that is sufficient to solidify the helium. The effective mass of the positive ion, which is the sum of the mass of the solid region enhanced by a hydrodynamic contribution due to the surrounding fluid, is about 30 m_4 at low temperature, where m_4 is the mass of a helium atom, and increases with increasing temperature for reasons that are not fully understood.

The negative 'ion' consists of an electron in an otherwise empty bubble, this being a state of lower total energy than if the electron were to enter the bulk helium. The radius of the bubble is determined, essentially, by a balance between the energy of the bubble and the zero-point energy of the electron, and adopts a value of about 1.7 nm. The effective mass of the bubble is entirely hydrodynamic, the mass of the electron itself being negligible; it is found to be independent of temperature and equal to 237 m_4.

The experimental results discussed in this paper were all obtained using positive ions. However, for the purposes of the work described here the detailed structure of the ions is unimportant. We shall treat them as point charged particles, with the appropriate effective mass.

Let us consider now the mechanism by which the ions may be trapped below the free surface of superfluid helium. The temperature is assumed to be low, so there is effectively a vacuum above the surface. An ion situated below the helium surface experiences a repulsive interaction with the polarization charge density that it induces on the helium–vacuum boundary, the effect of which can be represented by a suitable image charge. If an external electric field is applied in the vertical direction, the ion then experiences a net potential which has a minimum, within which the ion may be trapped, at a depth below the helium surface of typically 50 nm. This potential well can be filled with ions up to an areal number density of typically 10^{12} m^{-2}, using a suitable fringing field to confine the ions horizontally. In practice, a circular sheet of ions of radius about 13 mm is confined by electric fields which are provided by the application of appropriate potentials to a set of surrounding electrodes, shown schematically in figure 1. The equilibrium density profile in the pool is determined by electrostatics (see the discussion by Barenghi *et al* 1991). It is found that the density is almost independent of radius except within a distance h of a well-defined edge at which the radial component of the density gradient becomes infinite, where $2h$ is the separation of the horizontal confining electrodes situated above and below the ion pool. The pool is effectively two dimensional in the sense that vertical motion of the ions, which, at the temperatures concerned, is thermally excited over a range of quantum states within the trapping potential well, has an amplitude much less than the inter-ion spacing. Horizontal motion of the ions is much less restricted, and governed by a classical Coulomb ionic interaction, which is screened by the presence of the confining electrodes. In order to excite resonant motion of the ions, alternating potentials of variable frequency may be applied, in addition to the steady confining potentials, to one or more of the surrounding electrodes. Resonant ionic motion is detected by measuring the charge induced on another electrode, as illustrated in figure 1.

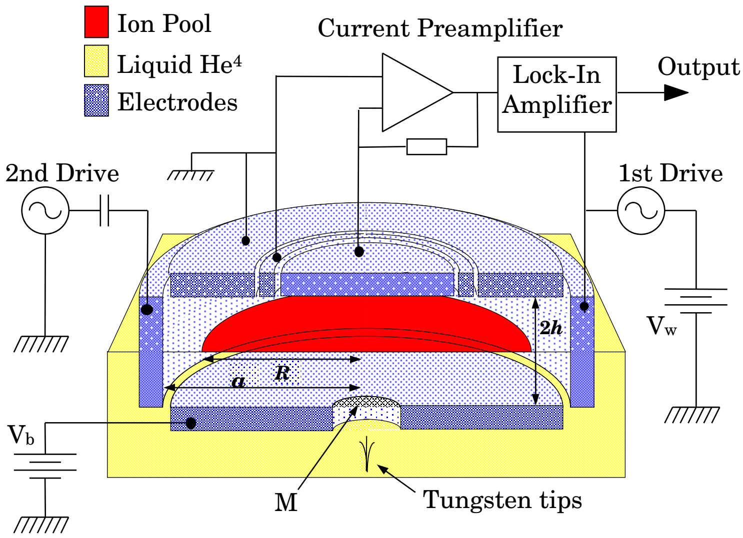

Figure 1. A schematic diagram of the electrode assembly and circuit used to study ion pools. The electrodes are shaped in the form of a pill box, which is half filled with liquid helium. M indicates a mesh grid incorporated into the bottom electrode, which allows access by the ions into the electrode assembly. Typically $R = 13$ mm, $a = 15$ mm, $h = 1.5$ mm; $V_w = 40$ V, $V_b = 10$ V.

As we have stated, our experiments are carried out in the temperature range 10–200 mK. The electrode assembly is placed inside an experimental cell, which can then be filled to the appropriate level with liquid helium; the cell is attached to the mixing chamber of a dilution refrigerator. The helium in the cell is isotopically pure, so at such temperatures the superfluid helium provides a very clean background medium, imposing little dissipation on the motion of the ions; indeed, at the lowest temperatures the ionic motion is damped only by the ripplons on the liquid surface. This affords the study of the resonant motion of the ions, which we now turn to discussing.

3. Magnetoplasma modes

Two-dimensional plasma modes were first observed in the related system of electrons trapped above the surface of helium by Grimes and Adams (1976), and in the ion system by Ott-Rowland *et al* (1982). These modes involve the collective longitudinal motion of the ions in the plane of the pool. In the simplest theoretical treatment of these modes, detailed by Barenghi *et al* (1991), which is sufficient for gaining a qualitative understanding of their behaviour, the ion sheet is treated as having a uniform equilibrium density profile with an abrupt pool edge at which the density falls discontinuously to zero. For a bounded pool a discrete set of normal modes will exist, as only certain wavenumbers are allowed. Under the simplified theoretical approach, a plasma mode, specified by the indices (m, n), can then be represented by a fluctuation in the charge density of the form

$$\sigma_{m,n} = J_m(k_{m,n}r)\exp \mathrm{i}(m\theta - \omega t) \tag{3.1}$$

where we are using cylindrical polar coordinates (r, θ, z), the pool being in the plane $z = 0$ and centred at $r = 0$. The integer m determines the number of nodes in $\sigma_{m,n}$ in the azimuthal direction, n the number of nodes in $\sigma_{m,n}$ radially. The wavenumbers $k_{m,n}$ form a discrete set determined by a boundary condition that the radial component of the ionic displacement vanishes at the abrupt pool edge.

The frequencies of the plasma modes exhibit a curious behaviour in the presence of an applied vertical magnetic field. In the case of axisymmetric modes ($m = 0$), the boundary condition yields values of wavenumber that are independent of magnetic field, so the frequency of such a mode increases simply with increasing magnetic field. Non-axisymmetric modes behave in a more complicated way. In the absence of a magnetic field their frequencies are degenerate with respect to the sign of m. The application of a magnetic field lifts this degeneracy, and the boundary condition yields wavenumbers that are dependent on the magnetic field. The frequencies of all modes generally rise with increasing magnetic field. However, those modes with $n = 1$ and negative m actually fall in frequency with increasing field; interestingly, in sufficiently high magnetic field the wavenumbers of such modes become imaginary. This gives rise to a perturbation in charge density described by a modified Bessel function: the mode becomes increasingly localized to the pool edge as the magnetic field is increased. The mode is then known as an edge magnetoplasma wave, propagating around the edge of the pool within the localized region. The behaviour of the magnetoplasma mode frequencies is illustrated in figure 2, where a comparison is made between the measured frequencies of the experimentally observed modes (symbols) and those calculated using a simplified theoretical treatment which is subject to the assumptions described above (broken curves). It can be seen that this theory describes only qualitatively the behaviour of these modes. Much attention has been paid recently to the development of a more thorough analysis (details are given in Elliott *et al* 1997) which takes correct account of the electrostatics in the pool and of the inhomogeneity in the ionic density near the pool edge. It has been shown that a movement of the pool boundary accompanies the plasma mode, giving a reduction in the mode frequencies; the calculated mode frequencies, shown in figure 2 (solid curves), are found to be in excellent agreement with the experimental results.

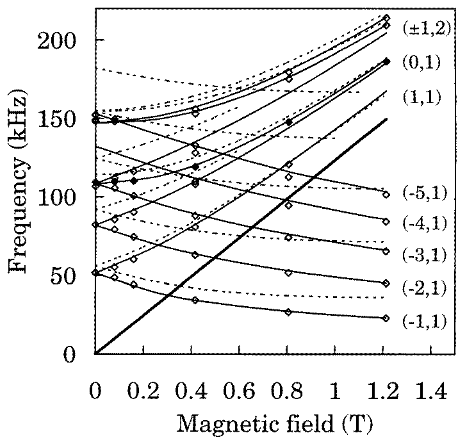

Figure 2. Measured frequencies of the conventional magnetoplasma modes plotted against magnetic field. Broken curves: simple theory with a rigid pool boundary; solid curves: theory taking correct account of the behaviour of the pool edge. The data are for a pool of areal density 6.56×10^{11} m^{-2} at 37 mK.

A further important consequence arises if account is taken of the fact that the edge of the pool is not strictly abrupt: the existence of a new family of edge magnetoplasma modes, predicted to exist by Nazin and Shikin (1988). These modes are localized within the region of inhomogeneity in the ionic density at the pool edge and, unlike the conventional edge magnetoplasma modes described previously, involve spatial oscillations in the perturbed charge density in the radial direction within the region of localization. The frequencies of these 'multipole' edge magnetoplasma modes, which are typically 5 kHz, depend on the magnetic field in a characteristic way, through which they were identified (Elliott *et al* 1995).

The multipole edge modes, and also the conventional non-axisymmetric magnetoplasma modes, should not actually be generated and detected by direct electrostatic coupling to a surrounding electrode assembly which has circular symmetry. It turns out that, in practice, the experimental cell does not have perfect symmetry, probably due, for example, to slight misalignment of the electrodes and the liquid surface. The resulting small electrostatic coupling is sufficient to allow very inefficient generation and detection of the different families of non-axisymmetric modes. However, while we rely on this mechanism for their generation, the reliable detection of these modes has rested on the development of an indirect 'double-drive' detection technique, which exploits a non-linear coupling which exists between different modes of the pool. In this technique the response of an axisymmetric magnetoplasma mode, which is easily generated and detected in our experimental cell, is studied in the presence of a second mode which is simultaneously excited at an appropriate frequency using a drive of rather high amplitude applied to one of the electrodes surrounding the pool. In the presence of the simultaneously excited second mode, it is found that the response of the axisymmetric magnetoplasma mode changes, primarily by a reduction in its resonant frequency. The effect is illustrated in figure 3, which shows the observed response of the $(m = 0, n = 1)$ axisymmetric magnetoplasma mode, driven and detected at its resonant frequency, as a second drive is swept through a range of frequencies. The rich spectrum observed shows several multipole edge magnetoplasma modes, and the lowest-frequency conventional edge magnetoplasma mode (largest peak). The observed modes are seen to be very clearly defined, illustrating the great sensitivity of this technique; this is particularly true at low temperatures where the (0, 1) magnetoplasma mode has a very high Q and is therefore very sensitive to small changes in resonant frequency. As we shall see in the following sections, the double-drive technique has been essential to the study also of other important characteristic modes of the ion pool system.

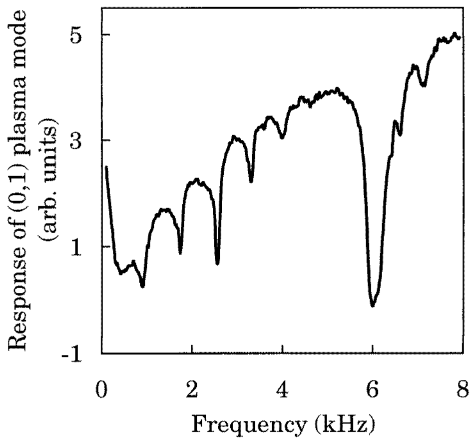

Figure 3. A typical response of the (0,1) plasma mode when a second drive is swept through the frequency range of the multipole edge magnetoplasma modes. The largest peak is the lowest-frequency conventional edge magnetoplasma mode. A pool of areal density 8.8×10^{10} m^{-2} at 60 mK, in a magnetic field of 1.2 T.

4. Shear modes

As we have noted previously, pools of ions, and also electrons, at the surface of helium are expected to form a two-dimensional Coulomb crystal at low temperature (Crandall and Williams 1971). This crystallization was first observed in the electron system above the helium surface (Grimes and Adams 1979). While the magnetoplasma modes that we have so far discussed in this paper are present in both the fluid and crystalline phases of the ion pool, the crystalline phase supports, in addition, resonant shear modes whose behaviour is governed by the elastic modulus of the crystal. A study of the shear modes can therefore serve to provide information regarding the mechanical properties of the ion crystal.

As we have explained, magnetoplasma modes couple electrostatically to the surrounding electrode assembly, since these modes involve fluctuations in the charge density in the pool, making their study rather simple. Pure shear modes involve no such fluctuation, so their generation and detection is more problematic. The difficulty of generating shear modes in the ion crystal may be overcome by applying to the pool a steady vertical magnetic field, as was done by Deville *et al* (1984), who observed the propagation of shear modes in the system of electrons above the helium surface. This procedure introduces a coupling between the shear modes and the magnetoplasma modes through the action of the Lorentz force, leading to the formation of two hybrid modes. The implications of this coupling are detailed in Appleyard *et al* (1995); its effect on the behaviour of the two types of mode turns out to be rather small, so we continue to label them as magnetoplasma modes and shear modes even in the presence of a magnetic field. However, a small longitudinal component which is gained by the shear modes is sufficient to permit their generation electrostatically, by again applying an appropriate alternating potential to one of the surrounding electrodes of the experimental cell. While this technique allows the effective generation of shear motion of the ions, it is not sufficient to permit the detection of the resulting transverse response of the pool. Shear modes may be observed rather easily, however, by again making use of the double-drive technique, in the same manner as discussed previously in relation to the detection of the different families of non-axisymmetric magnetoplasma modes. Shear mode detection by this procedure is illustrated in figure 4, which shows the response of the (0, 1) magnetoplasma mode, driven on resonance, when a second drive of relatively large amplitude is swept through the range of frequency at which the shear modes are expected to lie. The resonant frequencies of the detected modes and their dependence on temperature are found yield a value for the elastic modulus of the ion crystal that is consistent with theoretical prediction (Bonsall and Maradudin 1977) and numerical simulation (Morf 1979), which furthermore demonstrates that the crystal lattice adopts a hexagonal structure.

The linewidths of the observed shear modes are found to exhibit an interesting behaviour, which may allude to internal friction in the ion crystals. The attenuation of the shear modes must be due in general to a combination of dissipative effects within the ion system and the damping associated with the fact that each individual ion has a finite mobility arising due to interactions with the thermal excitations within the helium; more specifically, at the temperatures concerned, with ripplons on the helium surface. Measurements of shear mode linewidths may be obtained from double-drive spectra, such as that shown in figure 4. Clearly, such a measurement must be interpreted with care, due to the non-linearities inherent in the detection technique. Detailed studies of the double-drive technique have been carried out, allowing the extraction from observed spectra of the natural linewidths of the detected modes. Figure 5 illustrates the observed variation in the natural linewidth of the lowest-frequency axisymmetric shear mode with the amplitude of its drive for a typical pool held at two different depths below the helium surface. The observed linewidth is found to increase reversibly with

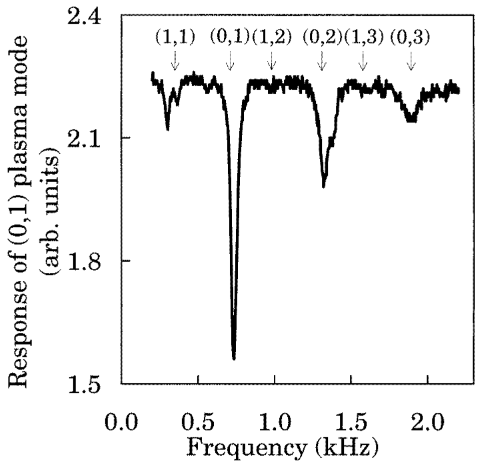

Figure 4. A typical spectrum of shear modes, observed using the double-drive technique. The arrows indicate the theoretical mode frequencies for the lowest few modes. A pool of areal density 7.51×10^{11} m^{-2} at 17 mK, in a magnetic field of 1.2 T.

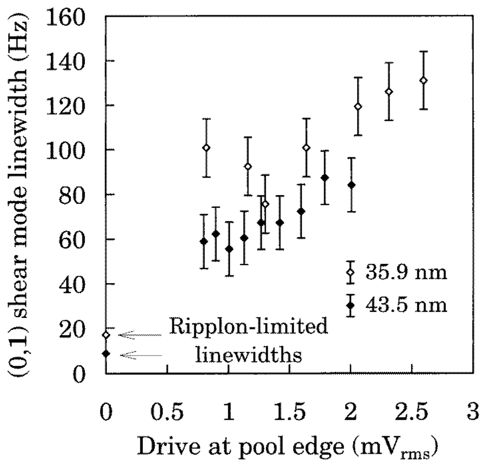

Figure 5. Observed variation in the linewidth of the lowest-frequency axisymmetric shear mode of a typical pool, at two different depths, on the amplitude of the drive at the pool edge. The expected linewidths due to ripplon damping alone are indicated.

drive level, and clear evidence is seen that it is significantly larger than would be expected if it were determined entirely by the ripplon-limited mobility, the relevant linewidths due to ripplon damping being indicated in the figure. We attribute the extra damping to internal friction within the crystal, arising from the motion of defects, although an additional contribution to the shear mode damping may also arise from the region of inhomogeneity in the ion density at the pool edge, which must be in a molten phase. When the crystal is strained, a finite time is required for defects present in the crystal to adjust to this change, and it is their subsequent motion which is believed to give rise to the additional dissipation within the crystal.

In addition to the revealing properties of the two-dimensional ion crystal exposed through a study of its resonant transverse modes, a study of the evolution of the transverse response through the melting transition may prove to be informative as regards our understanding of the nature of melting in two dimensions. The two-dimensional Coulomb crystal is believed to melt probably by a two-stage process, both stages involving a Kosterlitz–Thouless transition which is mediated by the dissociation of pairs of thermally excited defects in the crystal lattice (Kosterlitz and Thouless 1979, Halperin and Nelson 1978, Nelson and Halperin 1979, Young 1979). The first stage, at temperature T_m, involves a dissociation of pairs of dislocations, leading to a hexatic phase which exhibits order in the orientation of bonds between ions; the second stage, at temperature T_i, involves a dissociation of pairs of disclinations, leading to a fully disordered fluid phase. To determine whether this mechanism governs the melting transition is a major goal in our field of research, and an observation of the hexatic phase would provide overwhelming support for this view; an indicator of the character of the molten phase is the kinematic viscosity.

Above the melting transition, it is found that the resonant shear modes are replaced by a broad frequency response, such as would be characteristic of viscoelastic waves in a molten phase. Figure 6 illustrates a typical observed spectrum, obtained using the double-drive technique. The form of response observed is sensitive to the kinematic viscosity; the solid curve shown in the figure is a fit of the experimental spectrum to theory, using the kinematic viscosity as a fitting parameter. By studying the evolution, through the melting transition, of the shape of the observed response, it has been found that the kinematic viscosity exhibits an anomalous increase as T_m is approached from above and, furthermore, that this anomaly disappears as the level of drive imposed on the system increases. Firm conclusions based on these observations cannot yet be drawn. It seems to be the case that the drive level required to excite the response in the system is sufficient to cause, possibly, the deliberate separation of loosely bound pairs of dislocations prior to their natural dissociation. It is clear that further experiments are required with improved levels of sensitivity so that lower drive levels may be applied. However, the experiments certainly illustrate the value in using the transverse response as a probe of the nature of the molten phase, and this is clearly an area of promising future study.

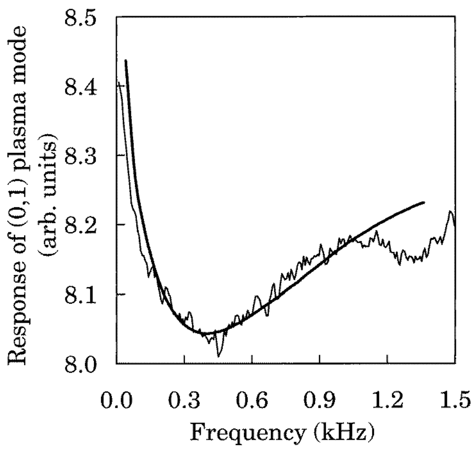

Figure 6. A typical viscoelastic response, observed using the double-drive technique. The solid curve is a fit to theory, with the kinematic viscosity as an adjustable parameter. A pool of areal density 2.21×10^{11} m^{-2} and melting temperature 107.2 mK, at 115 mK in a magnetic field of 1.41 T.

5. Damage and annealing of the ion crystal

As we have seen in the previous section, shear modes in the crystal phase are damped to a significant extent by internal friction, arising from the motion of defects. This suggests that deliberate damage to the crystal, which may introduce an increased concentration of defects, ought to lead to enhanced shear mode damping. This is indeed found to be the case, the damage being imposed by applying to the ion crystal a drive of high amplitude that is swept through the range of frequency of the shear modes. The consequences of carrying out such a procedure are illustrated in figure 7, which shows a sequence of shear mode spectra observed using the double-drive technique as described previously. The upper spectrum in the figure is obtained for a carefully prepared crystal at a low level of shear mode drive, 20 mV_{rms} applied to the circular wall electrode surrounding the pool. At a time $t = 0$ the crystal is subjected to a high shear drive, corresponding to a drive level of 2 V_{rms} applied to the wall electrode, the frequency of which is swept through the range shown. The subsequent spectra are obtained for the low shear drive at the times indicated. The second spectrum, taken immediately after damage, shows that the shear modes have suffered a significant enhancement in their damping; indeed it can be observed that they have practically disappeared. This increase in mode attenuation is attributed to damage of the crystal. Furthermore, as can be seen from the following spectra in the sequence, the shear mode spectrum is found to recover over a period of many minutes. This recovery is ascribed to the subsequent annealing of the crystal as the defects disperse, through their diffusion presumably both to the edge of the crystal and to sites at which they may locate other defects with which to annihilate. The recovery time of the crystal is found to decrease with increasing temperature but, interestingly, its variation is rather gradual. In contrast, one might expect a process of annealing that involves the diffusion of defects through a crystalline

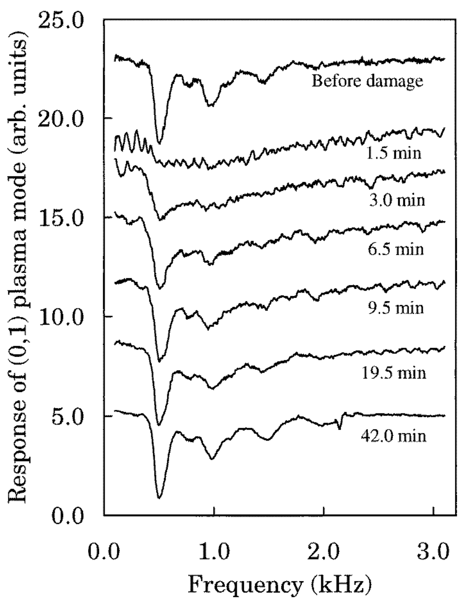

Figure 7. The time recovery of the shear spectrum, observed using the double-drive technique, after deliberate damage at a high shear drive amplitude. Spectra are obtained at low shear drive, at the times indicated after damage at $t = 0$. A pool of areal density 2.9×10^{11} m^{-2} at 17 mK, in a magnetic field of 1.35 T.

lattice to adopt an exponential dependence on temperature, reflecting a probability of defect hopping between lattice sites.

To interpret these observations we must understand the different ways in which a dislocation can move through the crystal lattice. Motion is of two types: 'glide' motion, which corresponds to the movement of a dislocation parallel to its Burgers vector, along a slip line, and 'climb' motion, which corresponds to motion out of a slip line. Climb of a dislocation requires the emission or absorption of vacancies or interstitials in order to progress, so motion of a dislocation is more likely to proceed by its glide. However, the diffusion of dislocations by glide alone cannot account for the observed recovery of the ion crystal, the predicted annealing rate being far too rapid and strongly dependent on temperature. We must therefore look to a mechanism by which the preferential glide motion of dislocations is impeded, thereby necessitating the involvement of much slower motion by climb. Presumably there are no impurities to obstruct the motion of dislocations, and therefore it is reasonable to suppose that interactions between dislocations in different slip lines may impede their glide motion. If these interactions can give rise to the formation of configurations of dislocation that are stable against glide, then climb would be required to explain the diffusion of dislocations in an annealing crystal. It is known that such configurations of dislocation can indeed be formed. Bruinsma *et al* (1982) have explored this problem theoretically, in the context of liquid crystals. It was found that a grain boundary, which may be treated as a chain of dislocations, in the form of a closed square loop separating a rotated grain from the surrounding crystal, exhibits stability against the glide motion of its constituent dislocations. It is reasonable to suppose that damage in our ion crystals, due to the very strong excitation of the lowest-frequency axisymmetric shear mode, may adopt the form of a closed circular grain boundary within the crystal. We may then infer the requirement for dislocation climb to explain the annealing of a damaged crystal, where the recovery rate would be limited by the diffusion of vacancies or interstitials into the damaged region.

The origin of such vacancies or interstitials within the ion crystal is still under debate. Presumably, our annealing mechanism is not limited by concentrations of such defects as would exist in thermal equilibrium, since this would be again expected to give rise to an annealing rate which is strongly temperature dependent. As we have seen, this is not the case, which suggests that an equilibrium concentration of defects is maintained in the ion crystal in excess of that due to thermal excitation. The source of the apparent large defect concentrations remains unresolved; indeed, we cannot rule out the possibility that this is an intrinsic property of the two-dimensional Coulomb crystal that has so far eluded observation.

6. Capillary-wave crystallography

In our final topic of discussion we shall view the ion crystal from a different perspective, employing the surface ripplons as a probe of its structure. So far in our discussion we have not fully considered the influence of interactions between the ripplons and the ions. Such coupling does not lead to large changes in the dispersion relations of the modes that we have described, except for effects relating to the ripplon-limited mobility of the ions. However, significant effects due to ripplon coupling do exist, and turn out to be a useful tool for the observation of crystallization in the ion pools and for the study of the nature of this crystalline state.

Of particular interest to us is the existence, in the crystal phase, of a coupled ion–ripplon mode, predicted to exist by Shikin (1974) and Monarkha and Shikin (1974). They suggested that driven vertical oscillation of the ions would generate ripplons at the frequency of the applied drive and that, if the wavevector of the emitted ripplons is equal to a reciprocal-lattice vector of the ion crystal, then the ripplons generated by each ion would constructively interfere and give rise to a resonant response. Termed the *Shikin mode,* this response corresponds to the formation of a capillary standing wave in which there is an antinode with the same phase at all points where there is an ion. Its frequency, which we refer to as the *Shikin frequency* (typically a few MHz), is related to the reciprocal-lattice vector of the underlying crystal through the usual dispersion relation describing capillary-wave propagation for a deep liquid. Mellor and Vinen (1990) detected the Shikin mode in the ion crystal, thereby demonstrating its crystallization, by measuring an enhancement in the absorption of energy from the driving electric field at the Shikin frequency. This absorption turns out to be very small, making such an observation of the Shikin mode rather difficult. In addition, the observed peak in the absorption signal at the Shikin frequency was found to be very broad, contrary to expectations and probably arising due to the high drive levels necessary to detect a signal imposing damage to the crystal.

Fortunately, the Shikin mode may be easily detected by an indirect technique, by observing its effect on the attenuation of a simultaneously driven magnetoplasma mode. In addition, as we shall explain, it turns out that this indirect method of detection gives a more advanced understanding of the mechanism accompanying the excitation of the Shikin mode. We arrange to study the response of the (0, 1) plasma mode in the presence of a simultaneous rf drive, termed the Shikin drive, which is close to the Shikin frequency. The (0, 1) plasma mode is driven at low amplitude, by applying an alternating potential to the wall electrode surrounding the ion crystal, and its response is detected in the usual manner, through lock-in detection at the frequency of the (0, 1) plasma mode drive. The rf Shikin drive, which has higher amplitude, is applied to the outer electrode of the upper part of the cell assembly.

Figure 8 shows the observed in-phase response of the (0, 1) plasma mode in the presence of a simultaneously excited Shikin mode. The (0, 1) plasma mode response is measured at fixed frequency, referenced from the plasma mode driving signal, while the rf Shikin drive is swept across a range of frequency close to the Shikin frequency. The figure is then assembled by incrementing the frequency of the plasma mode driving signal through the resonant frequency of the (0, 1) plasma mode. Well defined features in the response can be observed. A sharply defined feature, which is primarily an increase in the plasma mode frequency, can be seen in the centre of the figure, at an rf drive frequency which we interpret as the Shikin frequency.

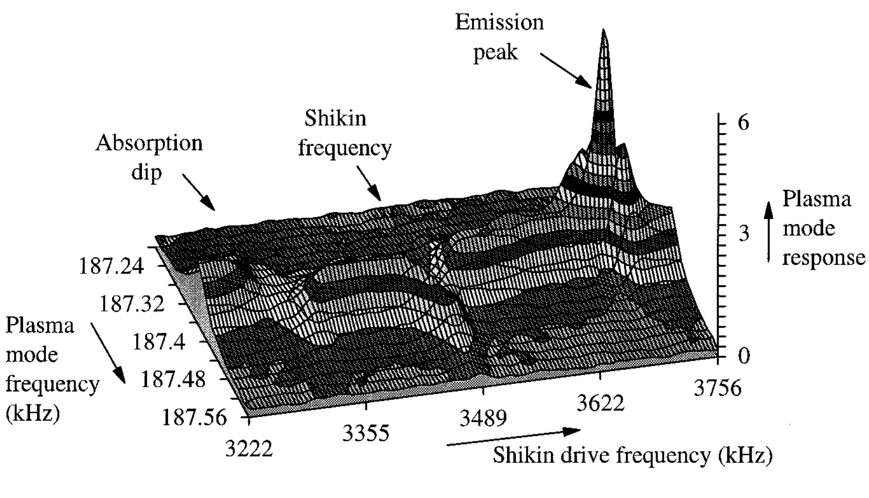

Figure 8. In-phase response of the (0, 1) plasma mode observed in the presence of the lowest-frequency Shikin mode. A pool of areal density 7.14×10^{11} m^{-2} and melting temperature 193 mK, at 36 mK in a magnetic field of 1.21 T.

This interpretation follows from the fact that if the ionic density is derived from the measured frequency, through the reciprocal-lattice vector, then it is found to be consistent with that obtained independently from analysis of the frequencies of the observed magnetoplasma modes. To each side of the central anomaly two further features of different character are observed. At a frequency equal to the sum of the Shikin frequency and the (0, 1) plasma mode frequency, a 'peak' in the (0, 1) plasma mode response can be seen, which implies a decrease in the plasma mode attenuation. At a frequency equal to the difference between the Shikin frequency and the (0, 1) plasma mode frequency, a 'dip' in the response is seen, implying an increase in the plasma mode attenuation.

A quantitative description of the features that have been described is rather involved; details will be given in a later publication. Within the scope of this paper we interpret these features only in as far as suggesting their origin. As already discussed, the excitation of the Shikin mode corresponds to the generation of capillary waves of wavevector equal to a reciprocal-lattice vector of the ion crystal, so a standing capillary wave is formed with each ion situated at an antinode. The observed shift in the (0, 1) plasma mode frequency is a consequence of the fact that the ripplons suffer a relatively small attenuation, so the standing capillary wave is unable to follow the motion of the ions as they oscillate at the plasma mode frequency. As the ions move in the plasma mode they will then experience an additional restoring force, arising from their interaction with the distorted helium surface, formed by the standing capillary wave. Calculations made to quantify this effect are found to be consistent with the observed magnitude of the frequency shift, and the fact that the plasma mode frequency increases verifies that the ions are indeed sited at antinodes, rather than nodes, of the standing capillary wave.

So far the Shikin mode has been regarded as a coupled ion–ripplon mode. To explain the features observed either side of the Shikin frequency, it is useful to adopt the language of x-ray and neutron scattering studies and view the Shikin mode as the 'Bragg' scattering of an incident electromagnetic wave, of essentially zero wavevector, into a capillary wave, of wavevector equal to the crystal reciprocal-lattice vector. We must then recognize that the production of capillary waves may be accompanied by the absorption or emission of plasmons or transverse phonons in the crystal, analogous to inelastic scattering processes seen in x-ray or neutron scattering. The observed dip at low frequency is interpreted as an extra absorption of energy from the driven (0, 1) plasma mode, when the generation of ripplons at the Shikin frequency is accompanied by the absorption of (0, 1) plasmons. Similarly, the peak observed at high frequency is interpreted as the stimulated emission of energy into the (0, 1) plasma mode, (0, 1) plasmon emission then accompanying ripplon generation.

Further study of the effects that we have described has been carried out, and proves to be revealing as regards our understanding of the ion crystal. If the rf Shikin drive is swept to higher frequency, for example, then it is possible to observe features analogous to those described above for higher-order Shikin modes, corresponding to the generation of ripplons with wavevectors equal to higher-order reciprocal-lattice vectors of the crystal. The frequencies of all of the observed Shikin modes form a pattern which illustrates very clearly the hexagonal lattice structure adopted by the Wigner crystal.

Perhaps the most interesting aspect of this work is the study of fundamental questions related to the understanding of the nature of crystallization in two dimensions. The question of the character of ordering in two dimensions is a subtle issue. Long-range translational order, which is familiar in a three-dimensional crystal, is inhibited in a two-dimensional system by the thermal excitation of long-wavelength phonons which give rise to fluctuations in the particle positions about their lattice sites. Nevertheless, we have noted that the ion system can form a crystal, and have indeed seen evidence to support this view. It turns out that the two-dimensional solid may be described as being one in which translational periodicity dies away only weakly with increasing distance (Mermin 1968), reflected in the algebraic decay of the appropriate Debye–Waller correlation function, with the result that a system of finite size may retain a non-zero degree of translational order. The two-dimensional solid should then give rise to Bragg-like peaks in the scattering structure factor, analogous to the absorption peaks seen by Mellor and Vinen (1990) and the features described above. A detailed analysis of the amplitude of the enhanced emission peak feature in figure 8 has been carried out. The intensity of this feature was found to decrease with increasing temperature and essentially disappear at the melting transition. This fall with increasing temperature is attributed to a loss of translational order arising from the thermal excitation of phonons in the crystal; presumably, close to the melting temperature, the dissociation of dislocation pairs would also give rise to a rapid loss in translational order as the solid melts. Measurements have been interpreted in terms of the structure factor associated with capillary-wave scattering, and are found to be consistent with the expected algebraic decay of the Debye–Waller correlation function, verifying that long-range translational order is indeed absent in two dimensions.

7. Concluding remarks

We have highlighted some of the areas of study in two-dimensional pools of ions trapped below the surface of superfluid helium that have been of interest to the Birmingham group over the past few years. The ion pool is a system which is really rather simple, and yet during this period has continued to reveal its interesting, and often surprising, properties. We hope that through this paper we have conveyed our enthusiasm for this subject, and illustrated that this is a very accessible system with which one can explore the fascinating behaviour of matter in two dimensions.

Acknowledgments

We would like to take this opportunity to acknowledge the work of Professor W F Vinen in his role as supervisor to the many research students who have participated in this research programme since its conception. We are grateful to Dr L Skrbek, who worked with us on the experiments described in this paper, and to E L Parker and G R Walsh for technical support. The work was supported by the Science and Engineering Research Council and the Engineering and Physical Sciences Research Council of the United Kingdom.

References

Appleyard N J, Elliott P L, Pakes C I, Skrbek L and Vinen W F 1995 *J. Phys.: Condens. Matter* **7** 8939
Barenghi C F, Mellor C J, Meredith J, Muirhead C M, Sommerfeld P K H and Vinen W F 1991 *Phil. Trans. R. Soc.* A **334** 139
Bonsall L and Maradudin A A 1977 *Phys. Rev.* B **15** 1959
Bruinsma R, Halperin B I and Zippelius A 1982 *Phys. Rev.* B **25** 579
Crandall R S and Williams R 1971 *Phys. Lett.* A **34** 404
Deville G, Valdez A, Andrei E Y and Williams F I B 1984 *Phys. Rev. Lett.* **53** 588
Elliott P L, Nazin S S, Pakes C I, Skrbek L, Vinen W F and Cox G F 1997 *Phys. Rev.* B **56** 3447
Elliott P L, Pakes C I, Skrbek L and Vinen W F 1995 *Phys. Rev. Lett.* **75** 3713
Grimes C C and Adams G 1976 *Phys. Rev. Lett.* **36** 145
Grimes C C and Adams G 1979 *Phys. Rev. Lett.* **42** 795
Halperin B I and Nelson D R 1978 *Phys. Rev. Lett.* **41** 121
Kosterlitz J M and Thouless D J 1979 *J. Phys. C: Solid State Phys.* **6** 1181
Mellor C J and Vinen W F 1990 *Surf. Sci.* **229** 368
Mermin N D 1968 *Phys. Rev.* **176** 250

Monarkha Yu P and Shikin V B 1974 *Sov. Phys.–JETP* **41** 710
Morf R H 1979 *Phys. Rev. Lett.* **43** 931
Nazin S S and Shikin V B 1988 *Sov. Phys.–JETP* **67** 288
Nelson J M and Halperin B I 1979 *Phys. Rev.* B **19** 2457
Ott-Rowland M L, Kotsubo V, Theobald J and Williams G A 1982 *Phys. Rev. Lett.* **49** 1708
Shikin V B 1974 *JETP Lett* **19** 335
Young A P 1979 *Phys. Rev.* B **18** 1855